11. N. A. Avdonin, "Selection of a numerical method for Stefan-type problems," Latviiskii Matematicheskii Ezhegodnik, No. 2, 5-21 (1966).
12. A. N. Tikhonov and A. A. Samarskii, Equations of Mathematical Physics [in Russian], Nauka, Moscow (1977).
13. M. W. E. Coney, "Calculations of rewetting of a hot surface," Nucl. Eng. Design, 31, 246-259 (1974).

ATOMIZATION OF A LIQUID BY A ROTATING ATOMIZER BLOWN WITH AN AIRFLOW

V. F. Dunskii and N. V. Nikitin

UDC 66.069.8

Monodispersed atomization of a fluid by a rotating atomizer blown by an airflow is experimentally studied. An equation, agreeing satisfactorily with the experimental data, is proposed.

Atomization of a fluid by a rotating disk or cone in monodispersed regimes has been examined in many papers. However, the case when air is blown coaxially past the disk has not been examined. This case is important for many practical applications. For example, when air is blown onto a disk, a turbulent air–drop spray, used for spraying commercially valuable plants with pesticides, is formed; in this case, it is important that the air flow not disrupt the monodispersed fragmentation of the liquid, i.e., the main advantage provided by the disk — the identity of the drops formed — must be conserved.

The experimental investigation was performed using the setup indicated schematically in Fig. 1. The rotating atomizer (cone) 1 with the drive from the electric motor 2 was placed in the outlet section of the exit nozzle 3, which was shaped like a converging tube and was oriented downwards. Air, blown by a fan, flowed through the nozzle 3 downwards, forming a turbulent free jet (Re = 10,600-67,000; the diameter of the nozzle was 42 mm). The velocity of the air in the exit section of the converging tube and in the constant velocity core, shown in Fig. 1 by the dashed lines, was constant and equalled u (with the exception of a small section of the aerodynamic wake after the atomizer). The air velocity decreased beyond the boundaries of this core.

The liquid was delivered to the atomizer by an insert pump 4 from the cylinder 5 with a constant low flow rate Q = 0.005 ml/sec and entered the rotating cone (diameter 25 mm) as a continuous jet.

We performed the experiments with liquid paraffin, diesel fuel, motor oil, and water. The physical characteristics of these liquids are indicated in Table 1.

The density of the test liquids varied insignificantly, the surface tension varied by a factor of 2.5, and the viscosity varied by a factor of 264.

A total of 61 experiments were performed. We shall examine the results of the first series of experiments, performed with liquid paraffin (25 experiments). We used a strobe tachometer to visualize the formation of the drops on the edge of the rotating cone.

The observations showed that when the velocity of the air flow u varied from 0 to 33 m/sec and the rotational frequency of the cone varied from 725 to 10,000 rpm (diameter of the cone 25 mm, fluid flow rate Q = 0.005 ml/sec), in atomizing liquid paraffin, the nature of the fragmentation of the liquid did not change and corresponded to the well-studie first monodispersed regime ([1-3]; Fig. 2): protuberances appeared on the liquid torus, from which branches formed; the branches grew, stretched out, and dropped off the edge in the form of approximately identical drops. Some displacement of the liquid torus downwards, toward the aerodynamic shadow formed by the cone (by 0.5-1 mm), was observed only for very low rotational velocities of the cone (725-1160 rpm) and appreciable air velocities (25-30 m/sec), but otherwise the nature of the drop formation remained, in this case, unchanged.

All-Union Scientific-Research Institute of Phytopathology. Translated from Inzhenerno-Fizicheskii Zhurnal, Vol. 44, No. 3, pp. 390-396, March, 1983. Original article submitted June 23, 1981.

 0022-0841/83/4403-0264$07.50

TABLE 1. Physical Characteristics of the Test Liquids

Liquid	Density ρ_L, g/cm³	Kinematic viscosity ν, cm²/sec	Surface tension σ, g/sec²
Liquid paraffin	0,870	1,49	30,5
Diesel fuel	0,892	0,028	30,6
Auto engine oil	0,897	2,64	29,5
Water	1,00	0,01	73,1

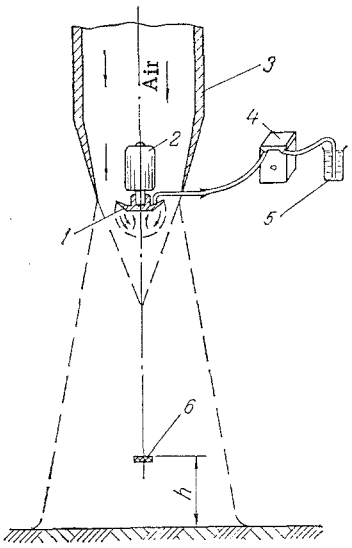

Fig. 1. Diagram showing the setup of the experiment.

Thus, in the entire range of variation of parameters investigated, an approximately monodispersed system of drops (and, as usual, much smaller satellite drops) were formed near the edge of the cone.

After the visual observations, we proceeded to count and measure the drops formed. For this, we collected the drops on a glass strip 6 (Fig. 1), placed near the axis of the spray at a height h above the floor. We chose the height h so that the velocity of the air in front of the strip 6 did not exceed 10 m/sec; in this case, the drops settled on the strip without breaking up. We covered the surface of the strip by a thin layer of silicone (the coefficient of spreading of the drops of liquid paraffin, diesel fuel, and motor oil ≈ 1.9). With the help of a slit shutter, we ensured an exposure time of the strip ~ 2 sec. After the drops were collected on the strip, we examined them under a microscope and counted and measured them. In the experiments with water, instead of the strip 6, we used a Petri dish with an immersion liquid (castor oil); the drops, settling on the surface of the liquid, submerged into it. After collecting the drops, we counted and measured them under a microscope.

To estimate the degree of monodispersity of the drops formed, we calculated the mean-square deviation a of their dimensions (by mass of the atomized liquid)* from the median size (by mass) d_{exp} and we determined the coefficient of variation $\alpha = a/d_{exp}$. The results of the experiments showed that as the velocity of the air u, blowing past the cone, increases, the mass-median diameter of the drops d_{exp} decreases.

To describe the experimental data quantitatively, we derived a semiempirical working equation. For the condition for the main drop to break away from the edge of the rotating atomizer in the "first" monodispersed atomization regime, we used the equality of the forces acting on the drop, but in this case, in the presence of air blown past the atomizer, the

* $a = \sqrt{\frac{\Sigma \Delta g_i (d_i - d\exp)^2}{\Sigma \Delta g_i}}$, where Δg_i is the weight of the liquid, situated in the i-th fraction of the drops with average size d_i.

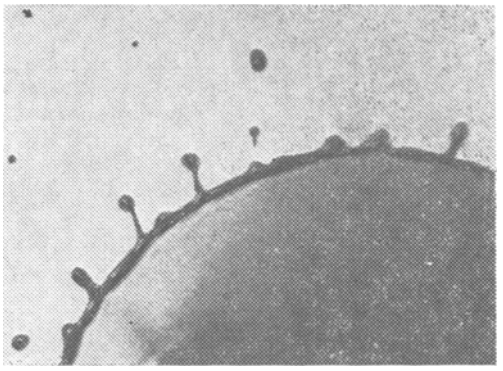

Fig. 2. First regime of monodispersed atomization of the liquid by the rotating disk.

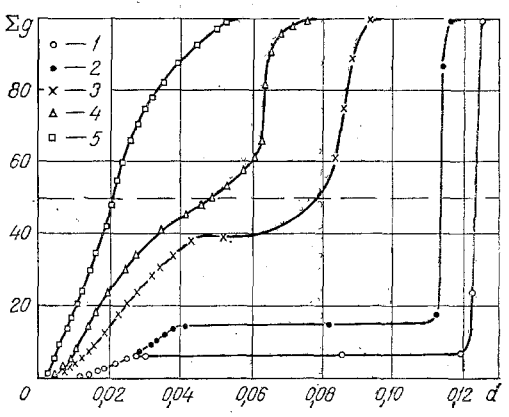

Fig. 3. Comparison of integral curves of drop-size distributions in experiments No. 2-6 (n = 890 rpm): 1) u = 6 m/sec; 2) 10.5; 3) 15; 4) 20; 5) 25. Σg, %; d, cm.

aerodynamic force A was added to the usual surface tension force $S \sim \pi d\sigma$ and centrifugal force $B=\frac{\pi d^3}{6}\rho_L R\omega^2$ and in view of the fact that these forces act in different direction, it was assumed that they were geometrically equal:*

$$S = \sqrt{B^2 + A^2}. \tag{1}$$

It was assumed that the aerodynamic force corresponds to a stationary unperturbed air flow past a sphere, i.e., that $A=\frac{\pi d^2}{4}\frac{\rho a u^2}{2}K$, where the drag K is a function of the Reynolds number.

Substituting the values of S, B, and A into equality (1), we obtain the working equation for determining d:

$$d=\frac{3}{4\sqrt{2}}\frac{\rho_a u^2 K}{\rho_L R\omega^2}\sqrt{\sqrt{1+\left(\frac{4\sqrt{2}}{3}\frac{\rho_L R\omega^2}{\rho_a u^2 K}\right)^4}\left(\frac{6\sigma}{\rho_L R\omega^2}\right)^2-1}. \tag{2}$$

Comparison of the values of d_{exp} measured in the experiments with the values of d calculated using Eq. (2) showed that for small values of u (up to 10 m/sec), the ratio d_{exp}/d is close to 1, i.e., the diameters of drops d, calculated using Eq. (2), are close to the measured values for all rotational velocities of the cone studied. However, for higher air flow velocities (u > 10 m/sec), the values of d_{exp} became much smaller than d. It later turned

*It is assumed approximately that the centrifugal and aerodynamic forces B and A are oriented at an angle to one another.

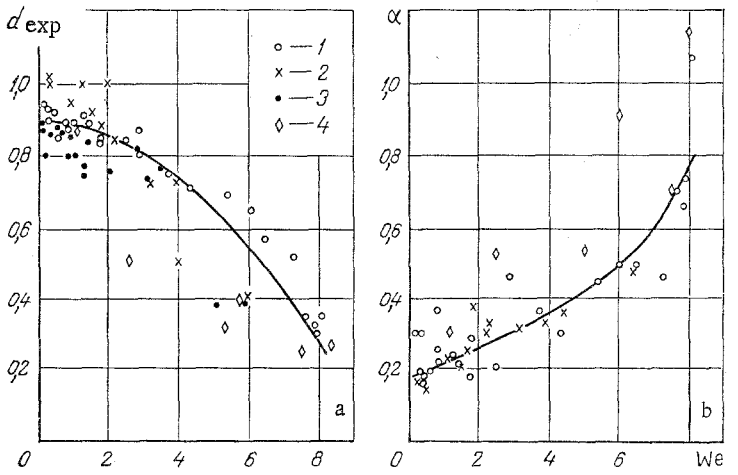

Fig. 4. Dependences $d_{exp}/d = f(We)$ and $\alpha = f(We)$ for different liquids: 1) liquid paraffin; 2) diesel fuel; 3) water; 4) motor oil.

out that for all values of the rotational frequency of the cone studied, as u increases, the coefficient of variation of drop sizes α increases, i.e., as u increases, there is a gradual transition from approximately monodispersed to polydispersed atomization.

This follows clearly from an examination of curves of drop size dispersions, obtained in each series of experiments, in which we varied the velocity u of the air flowing past the cone with other conditions remaining constant. These curves are compared for experiments with liquid paraffin, performed with n = 890 rpm and with other conditions remaining the same, but with the velocity u varying from 6 to 25 m/sec, in Fig. 3. It is evident from the graph that for u = 6 m/sec, the integral distribution curve has a form that is typical for the first monodispersed atomization regime [2, Fig. 21]: ∿94% of the mass of the liquid is contained in practically identical drops with diameter 0.120-0.125 cm and only 6% of the liquid is contained in fine satellite drops with diameters ranging from 0.010 to 0.026 cm. As the velocity u increases up to 10.5 m/sec, the nature of the curve remains the same, but the diameter of the main drops decreased (0.113-0.115 cm) in agreement with Eq. (2) and the total mass of the fine satellite drops increased somewhat (up to 15%) and their dimensions decreased (0.010-0.040 cm). At u = 15 m/sec, the shape of the distribution curves still remains close to the shape of the monodispersed curve, but the total mass of find drops increased to ∿40%, their range of sizes increased (0.004-0.045), and the quantity d_{exp} decreased to 0.077 (to a larger extent than the value of d according to Eq. (2); the quantity d_{exp}/d decreased to 0.638). At u = 20 m/sec, the process approached even more closely the polydispersed process and for u = 25 m/sec the atomization became practically polydispersed, the value of α reached 0.657 and, which is especially important, there are no drops larger than 0.05 cm. The shapes of the distribution curves in experiments with other liquids also changed in an analogous manner.

Based on these results, we propose that the reason for the gradual transition from monodispersed to polydispersed fragmentation with an increase in the velocity of the air flow u was the secondary fragmentation of the main drops by the air flow. Apparently, for moderate values of u, only part of the main drops, located under conditions that are most favorable for fragmentation, were subjected to secondary fragmentation; the relative number of main drops in this case decreased, while the relative number of the fine drops increased. As u increased, the fraction of main drops, subjected to fragmentation, increased and for a sufficiently high value of u, practically all main drops were fragmented, traces of monodispersity disappeared, and the system of drops became completely polydispersed.

This concept is supported by the absence of drops in the system not only of larger sizes than the main drops, but also drops equal in size to the main drops (for u = 25 m/sec, $d_{exp}/d = 0.315$), and the fact that visually, for these values of u, the main drops were observed to form (see above), while they were not observed among drops deposited on the glass.

In the experiments with the remaining test liquids, results similar to the results shown in Fig. 3 were obtained (in the experiments with water, the fine satellite drops were not included, since their sizes greatly decreased due to evaporation before falling into the immersion liquid).

The condition for secondary fragmentation of drops in the air flow is customarily characterized by the magnitude of Weber's number:

$$We = \rho_a u^2 d / 2\sigma.$$

The results of the experiments are presented in the form $d_{exp}/d = f(We)$ in Fig. 4a and in the form $\alpha = f(We)$ in Fig. 4b.

As can be seen from Fig. 4a, for small values of We of the order of 0-2, the values of d_{exp}/d for all test liquids are close to unity (they vary from 0.74 to 1.03), i.e., the measured values of the median (by mass) diameter of drops d_{exp} is close to the values of d, calculated from Eq. (2). As We increases, in the region We > 2, the values of d_{exp}/d rapidly decrease and attain 0.24-0.35 for We = 7.6-8.4.

According to Fig. 4b, as We increases, the coefficient of variation of drop size α increases rapidly: from 0.14-0.36 with $We \leqslant 1$ to 0.66-1.03 with We = 8, i.e., as We increases, the degree of polydispersity of the system of drops increases rapidly.

These results must be viewed as quantitative confirmation of the model of secondary fragmentation of drops in an air flow blown past the atomizer as the reason for the gradual (with increasing u) transition of the monodispersed system of drops into a polydispersed system; secondary fragmentation began (under the given experimental conditions) at $We \approx 2$ and was largely completed at $We \approx 8$.

It should be noted, however, that the data presented are only indirect data and not a direct indication of the presence of secondary fragmentation under the given conditions. For this reason, until direct proof is obtained, secondary fragmentation of drops under the given conditions must be viewed as a hypothesis.

Furthermore, the critical values of Weber's number obtained differ from some of the values occurring in the literature. This should be explained by the fact, as noted in [1, 4], that the critical value of Weber's number, characterizing secondary fragmentation of drops, cannot be viewed as a constant: secondary fragmentation is determined not only by the value of We, but also other criteria determining this process. For this reason, the values of We_{cr} obtained by different authors under different conditions vary over wide ranges: according to the data presented in [4], from 1.7 to 7.5.

The critical value of Weber's number W_{cr} can depend on the viscosity of the atomized fluid. In order to clarify this problem, Fig. 4a compares the results of experiments performed both with low viscosity liquids (water, diesel fuel) and with a very viscous liquid (motor oil); the viscosity of the mineral liquids used varied by a factor of 94, while the remaining characteristics (σ, ρ_L) were close to one another. In Fig. 4a, in comparing the data obtained with different liquids, some separation of points is observed, but it is not possible to discern the effect of the viscosity of the liquid: the data for motor oil are close to the data for water and for diesel fuel. Therefore, the problem of the effect of the viscosity of the liquid on the process examined, just as the reasons for separation of the data (spread in the points) in Fig. 4a, remain open.

Thus, for We > 2, i.e., for relatively large size of the main drops and with considerable velocities u of the air flow, the monodispersed system of main drops, formed by the rotating atomizer in the first monodispersed regime [1-3], goes over into a polydispersed system, apparently, due to secondary fragmentation of drops by the air blown past the atomizer. For practical purposes, this means that in this case the main advantage of the rotating atomizer, namely, the monodispersed fragmentation of the fluid, is lost. In order to avoid this harmful phenomenon, the process must be performed with Weber numbers $W_{cr} \geqslant 2$.

NOTATION

A, B, and S, aerodynamic force, the centrifugal force, and the surface tension force; d_{exp} and d, median (by mass) measured and computed drop diameters; Q, ρ_L, σ, ν, flow rate, density, surface tension, and kinematic viscosity of the liquid; ρ_a, ν_a, u, density, kinematic viscosity, and the velocity of air; R, ω, radius and the angular rotational velocity of the disk; Re and We, Reynolds and Weber numbers; a, mean square deviation; α, coefficient of variation.

LITERATURE CITED

1. Yu. F. Dityakin, L. A. Klyachko, B. V. Novikov, and B. I. Yagodkin, Atomization of Liquids [in Russian], Mashinostroenie, Moscow (1977).
2. V. F. Dunskii, N. V. Nikitin, and M. S. Sokolov, Monodispersed Aerosols [in Russian], Nauka, Moscow (1975).
3. W. H. Wlaton and W. C. Prewett, "The production of sprays and mists of uniform drop size by means of a spinning disk," Proc. Phys. Soc. (London), 62B, 341-347 (1949).
4. V. F. Dunskii and N. V. Nikitin, "Atomization of liquids by a rotating disk and the problem of 'secondary' fragmentation of drops," Inzh.-Fiz. Zh., 9, No. 1, 54-60 (1965).

EVALUATION OF SWIRL RATIO AND KARMAN NUMBER FOR VORTICES

V. A. Bobr, I. Z. Gabdullin,
V. I. Kalilets, A. A. Sobol'ev,
and A. D. Solodukhin

UDC 532.517.4

Results of calculations are shown pertaining to similarity numbers for vortex tubes. Experimental data pertaining to various prototype and model studies are investigated.

There are now several experimental test stands available for simulation of streams whirled about the vertical axis [1]. However, only a few studies have been made concerning the selection of similarity numbers for such streams. Here estimates for some characteristic cases of whirled jet flow induced by various types of vortex generators will be given.

Following an analysis of the Navier–Stokes equations of motion as basis, we introduce the dimensionless parameter S representing the vortex ratio [1]

$$S = \frac{\pi v r^2}{Q}. \tag{1}$$

In turbulent streams during rotation there appear secondary convection currents. Their effect on the principal motion cannot be disregarded here. Using the method of scale conversions, we reduce the Reynolds equations to the dimensionless form

$$\frac{\partial \mathbf{v}_0}{\partial t} + (\mathbf{v}_0\nabla)\,\mathbf{v}_0 = -\frac{1}{\rho}\nabla P_0 + \nu\Delta\mathbf{v}_0 + \operatorname{div}(-\overline{\mathbf{v}'\mathbf{v}'}).$$

The scale for nondimensionalizing the fluctuation velocities we select according to Truesdell [2], viz.

$$\mathbf{v}' = \sqrt{\frac{\mu\varepsilon}{\rho}}\,\hat{\mathbf{v}}'. \tag{2}$$

The variables we replace with normalized quantities $\hat{t}$, $\hat{\mathbf{r}}$, $\hat{\mathbf{v}}$, $\hat{P}_0$ as follows:

$$t = \frac{r_m}{v_m}\hat{t};\ \mathbf{r} = r_m\hat{\mathbf{r}};\ \mathbf{v} = v_m\hat{\mathbf{v}};\ P_0 = P\hat{P}_0;\ \rho = \rho_0\hat{\rho};\ P = \rho_0 v_m^2.$$

It has been proposed [2] that additional viscous stresses in a stream are proportional to the ratio of viscous friction forces to normal pressure forces. The selected scale (2) yields an expression for characteristic turbulent stresses in terms of a relation between these forces. Omitting the symbol of dimensionlessness in the notation, we obtain

$$\frac{\partial \mathbf{v}_0}{\partial t} + (\mathbf{v}_0\nabla)\,\mathbf{v}_0 = -\frac{1}{\rho}\nabla P_0 + \frac{1}{\mathrm{Re}}\Delta\mathbf{v}_0 + K\operatorname{div}(\overline{-\mathbf{v}'\mathbf{v}'}), \tag{3}$$

where $\mathrm{Re} = r_m v_m/\nu$ and $K = \mu\varepsilon/P$.

A. V. Lykov Institute of Heat and Mass Transfer, Academy of Sciences of the Belorussian SSR, Minsk. M. V. Lomonosov Moscow State University. Translated from Inzhenerno-Fizicheskii Zhurnal, Vol. 44, No. 3, pp. 396-401, March, 1983. Original article submitted January 26, 1982.

0022-0841/83/4403-0269$07.50